

Electrocatalytic CO₂ Reduction with a Homogeneous Catalyst in Ionic Liquid: High Catalytic Activity at Low Overpotential

David C. Grills,^{*,†} Yasuo Matsubara,^{*,†,‡} Yutaka Kuwahara,^{†,§} Suzanne R. Golisz,^{†,||} Daniel A. Kurtz,[†] and Barbara A. Mello[†]

[†]Chemistry Department, Brookhaven National Laboratory, P.O. Box 5000, Upton, New York 11973-5000, United States

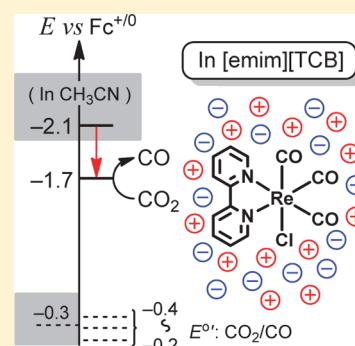
[‡]PRESTO, Japan Science and Technology Agency (JST), Chiyoda-ku, Tokyo 102-0076, Japan

[§]Department of Applied Chemistry and Biochemistry, Graduate School of Science and Technology, Kumamoto University, 2-39-1 Kurokami, Chuo-ku, Kumamoto 860-8555, Japan

S Supporting Information

ABSTRACT: We describe a new strategy for enhancing the efficiency of electrocatalytic CO₂ reduction with a homogeneous catalyst, using a room-temperature ionic liquid as both the solvent and electrolyte. The electrochemical behavior of *fac*-ReCl(2,2'-bipyridine)-(CO)₃ in neat 1-ethyl-3-methylimidazolium tetracyanoborate ([emim][TCB]) was compared with that in acetonitrile containing 0.1 M [Bu₄N][PF₆]. Two separate one-electron reductions occur in acetonitrile (−1.74 and −2.11 V vs Fc^{+/0}), with a modest catalytic current appearing at the second reduction wave under CO₂. However, in [emim][TCB], a two-electron reduction wave appears at −1.66 V, resulting in a ~0.45 V lower overpotential for catalytic reduction of CO₂ to CO. Furthermore, the apparent CO₂ reduction rate constant, *k*_{app}, in [emim][TCB] exceeds that in acetonitrile by over one order of magnitude (*k*_{app} = 4000 vs 100 M^{−1} s^{−1}) at 25 ± 3 °C. Supported by time-resolved infrared measurements, a mechanism is proposed in which an interaction between [emim]⁺ and the two-electron reduced catalyst results in rapid dissociation of chloride and a decrease in the activation energy for CO₂ reduction.

SECTION: Surfaces, Interfaces, Porous Materials, and Catalysis

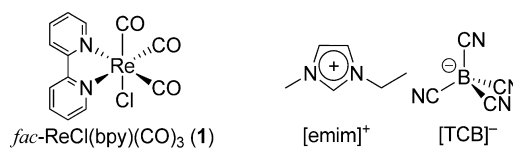


The activation and conversion of CO₂ into clean fuels and precursors, for example, CO, formate, or CH₃OH, is a promising strategy in ongoing efforts to achieve a sustainable global energy technology.^{1–5} Because CO₂ is thermodynamically stable, its conversion into higher-energy molecules is challenging. Many electrocatalysts that facilitate such processes have been developed, ranging from heterogeneous metals or alloys on electrode surfaces, to homogeneous transition-metal complexes.^{6–8} However, problems often encountered include low rates of catalysis, catalyst instabilities, and excessive energy consumption due to high overpotentials (η).⁹ Although catalysts that overcome these issues have been reported,^{10,11,6} their activities still fall short of what would be required for large-scale applications, and other problems persist, for example, the need for organic solvents or mercury electrodes. Therefore, further investigations of new strategies for the efficient electrocatalytic reduction of CO₂ are required.

Two intrinsic parameters define catalytic activity: turnover number (TON), that is, the number of moles of product per mole of catalyst, and turnover frequency (TOF). TOF is the TON per unit time and is related to the rate constant, *k*, of the catalytic reaction. Typically, within a given series of catalysts, TOF and η are linked, such that there is a linear increase in log(TOF) with η until a plateau is reached.^{12,10,13} However, the ultimate goal is to develop a catalyst that operates with a high TOF and low η .

Room-temperature ionic liquids (RTILs) are unique solvents that are emerging as superior alternatives to organic solvents for many applications.^{14–16} RTILs have also shown promise for improving the energy efficiency of heterogeneous electrocatalytic CO₂ reduction processes,^{17–22} although mechanistic details are not always clear and are still under investigation. Inspired by these reports, we sought to explore the effect of RTILs on the electrocatalytic reduction of CO₂ with homogeneous catalysts, focusing initially on *fac*-ReCl(bpy)-(CO)₃ (1; bpy = 2,2'-bipyridine; Chart 1), whose electrocatalytic

Chart 1. Structures of Re Catalyst (1) and [emim][TCB]



activity for the selective reduction of CO₂ to CO is already well understood in organic solvents, for example, acetonitrile (CH₃CN).^{23,24} Our RTIL of choice was [emim][TCB] (Chart 1)

Received: April 16, 2014

Accepted: May 15, 2014

Published: May 15, 2014

because it possesses a unique set of desirable properties for electrochemical CO₂ reduction^{25–27} compared with other RTILs.²⁸

To make a fair comparison between our results in [emim][TCB] and those in CH₃CN, we have estimated the formal thermodynamic potential, $E^{\circ'}$, for the reduction of CO₂ to CO (eq 1, where sol refers to a solvated species) in a variety of imidazolium-based RTILs (section B of SI). On the basis of a previous report,¹⁰ the standard thermodynamic potential, E° , in CH₃CN is estimated to be -0.28 V versus $\text{Fc}^{+/0}$ at pH 0 (obtained by subtracting²⁹ $+0.624$ V from the reported value¹⁰ of $+0.349$ V vs SHE), while in the RTILs, our estimates of $E^{\circ'}$ range from -0.15 to -0.39 V versus $\text{Fc}^{+/0}$ at $\text{p}[\text{H}^+] = 0$. Note that these $E^{\circ'}$ values were calculated from the formal redox potentials of H^+/H_2 in RTILs containing 1 M of acid derived from the RTIL anion, for example, HNTf_2 ($\text{p}[\text{H}^+] = 0$; $[\text{NTf}_2]^- = \text{bis}(\text{trifluoromethylsulfonyl})\text{imide}$) in NTf_2 -based RTILs.^{30,31} According to the strict definition of pH, that is, $\text{pH} = -\log_{10}(\gamma[\text{H}^+])$, where γ is the activity coefficient, the formal thermodynamic potential, $E^{\circ'}$, will be offset from E° by an amount equal to $RT\ln(\gamma)/F$. Unfortunately, the activity coefficients of H^+ in these RTILs are not currently available.^{32–35} However, because RT/F is only 0.026 V at 25°C , the extent of the potential shift is likely to be small compared with the range of $E^{\circ'}$ values we discuss. Thus, on average, $E^{\circ'}$ in the RTILs is similar to E° in CH₃CN (within ± 0.13 V). All reduction potentials in this study are reported versus the $\text{Fc}^{+/0}$ couple as an internal standard.³⁶

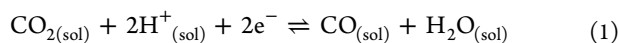


Figure 1 shows four typical cyclic voltammograms (CVs) of **1** in neat [emim][TCB] and in CH₃CN containing 0.1 M

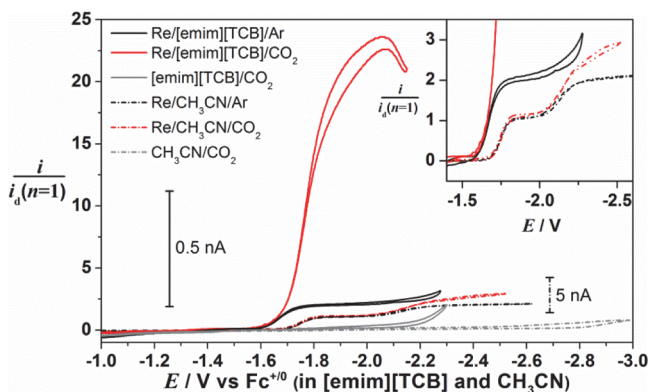


Figure 1. CVs of **1** recorded in [emim][TCB] (solid lines, 10 mV/s) and in CH₃CN containing 0.1 M [Bu₄N][PF₆] (dashed-dotted lines, 100 mV/s) using a UME (carbon fiber; effective diameter: 13 μm) after argon purging (black) and CO₂ purging (red) at $25 \pm 3^\circ\text{C}$. Currents, i , were normalized against a diffusion-limiting current defined by eq 2 for one-electron reduction. (See the text.) CVs in the absence of **1** under a CO₂ atmosphere are also shown in gray. $[\text{H}_2\text{O}] = 50$ mM in all cases and $[\text{1}] = 0.5$ mM for catalyst-containing solutions. Solid and dashed scale bars indicate the absolute current levels in [emim][TCB] and CH₃CN, respectively. Ohmic potential (iR) drop was not compensated for due to the extremely small currents involved.^{40,41} Inset: An expansion of the CVs showing the reduction steps in more detail.

[Bu₄N][PF₆] electrolyte, under argon and CO₂ atmospheres, using a carbon fiber ultramicroelectrode (UME) at low scanning rate. Under these experimental conditions, we could

observe sigmoidal voltammograms with limiting currents controlled by a constant thickness of the diffusion layer of the electroactive species on the electrode surface at sufficiently negative potential, that is, steady-state conditions. Because the diffusion coefficient, D_O , of **1** in [emim][TCB] was found to be approximately two orders of magnitude smaller than that in CH₃CN containing 0.1 M [Bu₄N][PF₆] ($D_O = (3.0 \pm 0.5) \times 10^{-7} \text{ cm}^2 \text{ s}^{-1}$ in [emim][TCB] and $(1.4 \pm 0.2) \times 10^{-5} \text{ cm}^2 \text{ s}^{-1}$ in CH₃CN/[Bu₄N][PF₆], determined by DOSY ¹H NMR measurements), the current in all CVs shown is normalized against the unit of the current function, i_d . i_d is defined by eq 2 for a reversible one-electron transfer under a diffusion mode governed by the shape of the UME (i.e., pseudohemispherical diffusion),³⁷ where r is the radius of the electrode, F is the Faraday constant, n is the number of electrons transferred (taken as 1 for this purpose), D_O is the diffusion coefficient of **1** (measured by NMR in this case), and C_O is the concentration of **1**. This normalization allows us to make a fair comparison between all CVs in terms of how many electrons are transferred in each reduction wave. We note that in organic solvents, diffusion coefficients, D , determined by NMR are typically almost identical to those determined by electrochemical methods,³⁸ and while there is some variation between NMR- and electrochemically-measured values of D in RTIL solvents, they are still reasonably consistent.³⁹

$$i_d = 4nFD_O C_O r \quad (2)$$

Four important features are observed in the CVs in Figure 1, as follows: (1) under an argon atmosphere, the first reduction potential of **1** in [emim][TCB] (-1.66 V vs $\text{Fc}^{+/0}$) is 80 mV more positive than that in CH₃CN (-1.74 V vs $\text{Fc}^{+/0}$); (2) in [emim][TCB], the second reduction of **1** occurs at the same potential as the first reduction ($i/i_d = 2$ for the reduction wave), whereas in CH₃CN there are two separate one-electron reduction steps at -1.74 V and -2.11 V versus $\text{Fc}^{+/0}$, each with $i/i_d = 1$ (see Figure 1 inset); (3) under a CO₂ atmosphere, in CH₃CN a modest catalytic wave is observed at the second reduction potential of **1** (onset at -2.11 V), which is known to be due to the selective catalytic two-electron reduction of CO₂ to CO,²³ while in [emim][TCB], a much larger catalytic current is observed at the first reduction wave (onset at -1.66 V) due to the observation described in feature 2;⁴² and (4) the potential at which the current reaches a plateau under CO₂ exhibits a ~ 0.45 V positive shift in [emim][TCB], similar to the shift of catalytic onset potential, thus indicating that the overpotential for CO₂ reduction is also reduced by ~ 0.45 V in [emim][TCB]. Importantly, we observed no Faradaic response in the absence of catalyst (gray curves in Figure 1).⁴³ The product obtained in [emim][TCB] was confirmed to be CO with a selectivity of $>98\%$ by bulk electrolysis experiments, where the Faradaic efficiency was $88 \pm 10\%$ (Figure S2 in the Supporting Information). In short, [emim][TCB] was observed to decrease the potentials required to both reduce **1** and for **1** to catalyze the selective reduction of CO₂ to CO compared with CH₃CN as a solvent.

The $+80$ mV shift of the first reduction wave of **1** in [emim][TCB] relative to that in CH₃CN could be due to several factors: the difference in ionic strength, a shift of the $\text{Fc}^{+/0}$ couple between CH₃CN and [emim][TCB], the dissimilarity of the diffusion coefficients of a charged species and its corresponding neutral species in an RTIL,³⁶ or a stabilization⁴⁴ of the one-electron reduced form of **1** by the imidazolium cation of [emim][TCB]. Because the ionic strength of [emim][TCB] (4.6 M) is much

greater than that of CH₃CN containing 0.1 M [Bu₄N][PF₆], we have measured CVs of **1** in CH₃CN containing [Bu₄N][PF₆] at concentrations of 0.1 and ~1.6 M (saturated conditions). These revealed a +70 mV shift in the first reduction potential versus Fc^{+/0} at the higher concentration. Thus, the +80 mV shift observed in [emim][TCB] is likely a result of the RTIL's high ionic strength. However, none of the previously mentioned factors explain the much larger positive shift of the second reduction wave so that it is coincident with the first reduction wave in [emim][TCB]. We have therefore investigated this behavior further.

It has previously been established that in CH₃CN the chloride ligand dissociates from **1** after either one-electron reduction or two-electron reduction²³ and that chloride ligand dissociation is a necessary step for catalytic CO₂ reduction to occur. However, the time scales for dissociation of chloride have not been measured. Our observation of catalytic CO₂ reduction beginning at the first reduction wave in [emim][TCB] therefore implies that in conjunction with the two sequential one-electron reductions of **1**, dissociation of chloride from the Re center also takes place at this potential. To clarify what happens at the first reduction wave in [emim][TCB], we measured CVs at various fast scanning rates ranging from 1 to 100 V/s under argon and CO₂ atmospheres, as shown in Figure 2.

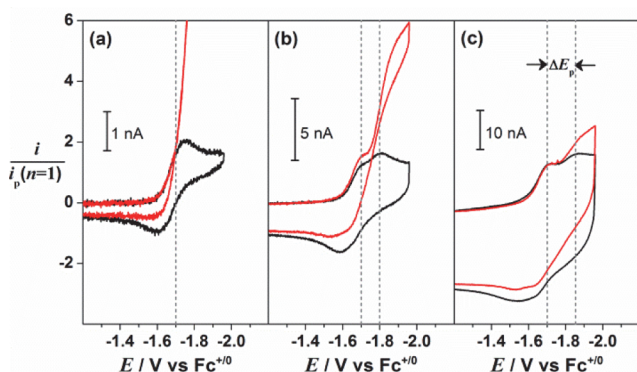


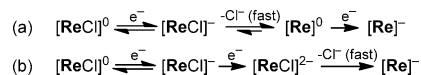
Figure 2. CVs of **1** (4 mM) in dry [emim][TCB] under argon (black) and CO₂ (red) atmospheres, measured using a UME (carbon fiber; effective diameter: 13 μm) at scanning rates of (a) 1, (b) 10, and (c) 100 V/s at 25 ± 3 °C. Currents (*i*) were normalized against a peak current defined by eq 3 for one-electron reduction. (See the text.) Gray dashed lines show the positions of the two reduction peaks, which are coincident in panel a. Scale bars show absolute current levels. Ohmic potential (*iR*) drop was not compensated for due to the extremely small currents involved.^{40,41}

The current in all CVs is again normalized against the unit of the current function defined by the Randles–Sevcik equation (eq 3) for a reversible one-electron transfer under linear diffusion mode, where *A* is the electrode surface area. Figure 2 is characterized by two important features, as follows: (1) At faster scanning rates, the single reduction wave breaks up into two reduction waves, with the second wave shifting to more negative potential and the first remaining at the same potential; the shift of the peak potential of the second reduction wave, Δ*E*_p, showed a dependence on the log of the scanning rate, log(*v*) (i.e., d(Δ*E*_p)/d(log(*v*)) ≈ −50 mV), which indicates that this electron transfer is quasi-reversible.^{45,46} (2) The catalytic wave was found to rise predominantly from the second peak, with its amplitude decreasing as the scanning rate increases.

$$i_p = 0.4463 \times nFAC_O\sqrt{D_Oa}; a = nFv/RT \quad (3)$$

On the basis of the theory of stationary electrode polarography,^{45,46} the separation of the first two reductions of **1** at high scanning rates suggests that there are two possible reaction mechanisms in [emim][TCB] (see Scheme 1), as

Scheme 1. Possible Pathways to the Two-Electron Reduced Catalyst in [emim][TCB]; Re = Re(bpy)(CO)₃

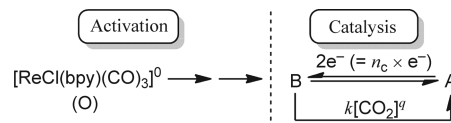


follows: (a) reversible electron transfer followed by very fast loss of chloride at the first reduction wave and then a quasi-reversible electron transfer at the second wave (*E*_r*C*_r + *E*_q) or (b) successive reversible and quasi-reversible electron transfers occur, followed by very fast loss of chloride (*E*_r + *E*_q*C*_i). Case a requires that the potential of the second electron transfer must be almost the same as the first (or more positive), and both cases require a chloride loss step that occurs on a time scale of <<1.5 ms (0.15 V peak separation at 100 V/s in Figure 2).

To help determine which of the two possible mechanisms in Scheme 1 is operating in [emim][TCB], we monitored the stability of the one-electron reduced catalyst, [ReCl(bpy)(CO)₃][−] (**1**[−]), by time-resolved infrared spectroscopy and found that chloride dissociation from **1**[−] occurs on a time scale of at least 20–30 s in [emim][TCB] (section D of SI), thus ruling out Scheme 1a on this voltammetric time scale. A similar slow loss of chloride from **1**[−] was also observed in CH₃CN. Therefore, it is likely that the positive shift of the second reduction wave in [emim][TCB] is due to a much faster loss of chloride from the two-electron reduced form of the catalyst, **1**^{2−} in [emim][TCB], compared with in CH₃CN (Scheme 1b). The C–H bonds on the imidazolium ring of the emim cation are known to strongly hydrogen bond to chloride anions in [emim]Cl,⁴⁷ and such an interaction with the chloride ligand of **1** may lead to an enhanced rate of chloride dissociation after the second reduction in [emim][TCB] compared with in CH₃CN. We note that it is unlikely that the heterogeneous electron-transfer rate constant is enhanced in [emim][TCB] because such rate constants are typically lower in RTILs compared with in CH₃CN.⁴⁸

Because catalytic CO₂ reduction is initiated at the second reduction of **1** in [emim][TCB] and CH₃CN, the same reaction model for the catalysis can be used in both solvents, as shown in Scheme 2, where it is assumed that CO₂ and water are

Scheme 2. Reaction Model for Kinetic Analysis



present in large excess compared with **1**, so that *k*[CO₂]^{*q*} can be considered to be a pseudo-first-order rate constant. This assumption is valid given the fact that we employed 50 mM H₂O in all experiments related to rate constant determination and the high solubility of CO₂ in [emim][TCB] (0.13 M/atm)²⁶ and CH₃CN/H₂O (0.26 M/atm).⁴⁹

The model in Scheme 2 can typically be classified as an *E*_r*C*_{cat} mechanism with activation. The ratio of the limiting current, *i*_c (current governed only by the rate constant of catalysis, *k*), and

the peak current, i_p (current governed only by diffusion of the singly reduced complex, that is, in the absence of catalysis), is defined by eq 4 (section E of SI). This ratio allows us to evaluate the apparent CO_2 reduction rate constant (k_{app}), which includes terms of the diffusion coefficients (D_A and D_B) of the species involved and which is related to the actual CO_2 reduction rate constant, k , by $k_{\text{app}} = (D_A/D_B)k$. In CH_3CN , the diffusion term is negligible because $D_A/D_B \approx 1$, that is, $k \approx k_{\text{app}}$. However, in $[\text{emim}][\text{TCB}]$, this will not be the case. For example, $D_A/D_B \approx 1.4$ was reported for the $\text{Fc}^{+/0}$ couple in various imidazolium RTILs,³⁶ and based on the diffusion coefficients measured for a series of Fe complexes with different charges in $[\text{bmpyrr}][\text{NTf}_2]$ ($[\text{bmpyrr}]^+ = 1\text{-butyl-1-methylpyrrolidinium}$),⁵⁰ we assume that D_A and D_B in $[\text{emim}][\text{TCB}]$ could differ by a factor of up to ~ 4 , that is, $D_A/D_B \leq 4$ and thus $k \geq k_{\text{app}}/4$.

$$\frac{i_c}{i_p} = \frac{n_c}{0.4463} \times \sqrt{\frac{RT}{Fv}} \times \sqrt{k_{\text{app}}[\text{CO}_2]^q}; k_{\text{app}} = \left(\frac{D_A}{D_B}\right)k \quad (4)$$

On the basis of eq 4, we examined the responses of the CVs of **1** to various concentrations of CO_2 ($[\text{CO}_2]$) and scanning rates (v) in $[\text{emim}][\text{TCB}]$ and CH_3CN in the presence of excess water (~ 50 mM). The current ratio measured in $[\text{emim}][\text{TCB}]$ was found to be proportional to both $[\text{CO}_2]^{0.5}$ and $(1/v)^{0.5}$. This observation allowed us to determine the reaction order with respect to $[\text{CO}_2]$ as one, and to calculate an apparent second-order rate constant for CO_2 reduction, $k_{\text{app}} = 4000 \pm 400 \text{ M}^{-1} \text{ s}^{-1}$ in $[\text{emim}][\text{TCB}]$ at a catalyst concentration of 2 mM in the presence of 50 mM H_2O at $25 \pm 3^\circ \text{C}$ (section G of the SI). The current ratio in CH_3CN was also found to be proportional to $(1/v)^{0.5}$, and assuming the reaction order with respect to $[\text{CO}_2]$ is one, we obtained $k_{\text{app}} = 100 \pm 20 \text{ M}^{-1} \text{ s}^{-1}$ in CH_3CN (section F of the SI). Under 1 atm of CO_2 , these values of k_{app} correspond to pseudo-first-order rates of 520 and 26 s^{-1} in $[\text{emim}][\text{TCB}]$ and CH_3CN , respectively. As previously discussed, the actual rate constant, k , of CO_2 reduction in $[\text{emim}][\text{TCB}]$ will be smaller than the apparent rate constant, k_{app} , by a factor of up to 4. However, it will still be much larger than that in CH_3CN (by a factor of at least $10\times$), implying that the RTIL helps to abate not only the electrochemical reduction potential of the complex (as previously described) but also the activation energy for the CO_2 reduction reaction.

The roles of $[\text{emim}]^+$ and $[\text{TCB}]^-$ in these experiments still have to be clarified. In preliminary experiments, we have found that a positive shift of the onset potential for catalytic CO_2 reduction by **1** is observed when 0.1 M of either $[\text{emim}][\text{TCB}]$ or $[\text{emim}][\text{tris(perfluoroethyl)trifluorophosphate}]$ is used as an electrolyte in CH_3CN . This implies that $[\text{emim}]^+$ is important for both the potential shifting and catalytic enhancement. In fact, we found that **1** in $[\text{emim}][\text{NTf}_2]$ shows similar catalytic activity to that in $[\text{emim}][\text{TCB}]$ (Figure S9 in the Supporting Information). We therefore believe that the effects we have observed are not limited to the specific combination of $[\text{emim}]^+$ and $[\text{TCB}]^-$. We note that previous work on other homogeneous CO_2 reduction catalysts in organic solvents has shown enhancement of catalytic currents^{51,52} or a positive shift of catalytic onset potential⁵³ upon the addition of alkali or alkaline earth metal cations to the solution. However, such effects have never been observed simultaneously, as with **1** in $[\text{emim}][\text{TCB}]$.

In future work, deployment⁵⁴ to an immobilized system would potentially allow the use of water as the major component of an electrochemical cell. For example, in another preliminary experiment, we have found that **1** dissolved in a droplet⁵⁵ (30 μL) of $[\text{emim}][\text{NTf}_2]$ placed on the surface of a working electrode can catalytically reduce CO_2 to CO in aqueous solution with a Faradaic efficiency of $71 \pm 10\%$ (Figure S11 in the Supporting Information).

In summary, we have found that using neat $[\text{emim}][\text{TCB}]$ as both the solvent and electrolyte results in a ~ 0.45 V lower onset potential and overpotential, η , for the electrocatalytic reduction of CO_2 to CO with $\text{fac-ReCl}(\text{bpy})(\text{CO})_3$ compared to in CH_3CN containing 0.1 M $[\text{Bu}_4\text{N}][\text{PF}_6]$. The use of $[\text{emim}][\text{TCB}]$ also increases the second-order rate constant, k , of CO_2 reduction by at least one order of magnitude. Supported by time-resolved infrared measurements, we have proposed a mechanism in which an interaction between the $[\text{emim}]^+$ cation and the two-electron reduced catalyst results in much more rapid dissociation of the chloride ligand compared with in CH_3CN and a lowering of the activation energy for the CO_2 reduction process. To the best of our knowledge, this is the first example of ionic liquid-enhanced electrocatalytic CO_2 reduction with a homogeneous catalyst, and given the extent of possible cation/anion combinations, this merits further studies of the enhancement of homogeneous electrocatalytic CO_2 reduction with RTILs.

■ ASSOCIATED CONTENT

Supporting Information

Full experimental details, additional electrochemical data, time-resolved infrared data, and complete ref 6. This material is available free of charge via the Internet at <http://pubs.acs.org>.

■ AUTHOR INFORMATION

Corresponding Authors

*E-mail: dcgrills@bnl.gov. Tel: +16313444332. Fax: +16313445815 (D.C.G.).

*E-mail: yasuo@bnl.gov. Tel: +16313444360. Fax: +16313445815 (Y.M.).

Present Addresses

^{||}S.R.G.: Chevron Products Company, Chevron U.S.A., Inc., 100 Chevron Way, Richmond, CA 94802-0627.

Notes

The authors declare no competing financial interest.

■ ACKNOWLEDGMENTS

This work was supported by the U.S. Department of Energy (DOE), Office of Basic Energy Sciences, Division of Chemical Sciences, Geosciences & Biosciences under contract # DE-AC02-98CH10886. Y.M. is supported by the PRESTO project: "Chemical Conversion of Light Energy" of the Japan Science and Technology Agency (JST). Y.K. is supported by the Japan Society for the Promotion of Science (JSPS) through the Strategic Young Researcher Overseas Visits Program for Accelerating Brain Circulation. D.A.K. and B.A.M. are grateful to the DOE and BNL's Office of Educational Programs for SULI internships. We thank Drs. Etsuko Fujita and Jim Wishart for helpful discussions and Dr. Dmitry Polyansky for help with LabVIEW programming for the TRIR data acquisition software.

REFERENCES

- (1) Sutin, N.; Creutz, C.; Fujita, E. Photo-Induced Generation of Dihydrogen and Reduction of Carbon Dioxide Using Transition Metal Complexes. *Comments Inorg. Chem.* **1997**, *19*, 67–92.
- (2) Benson, E. E.; Kubiak, C. P.; Sathrum, A. J.; Smieja, J. M. Electrocatalytic and Homogeneous Approaches to Conversion of CO₂ to Liquid Fuels. *Chem. Soc. Rev.* **2009**, *38*, 89–99.
- (3) Morris, A. J.; Meyer, G. J.; Fujita, E. Molecular Approaches to the Photocatalytic Reduction of Carbon Dioxide for Solar Fuels. *Acc. Chem. Res.* **2009**, *42*, 1983–1994.
- (4) Mikkelsen, M.; Jørgensen, M.; Krebs, F. C. The Teraton Challenge. A Review of Fixation and Transformation of Carbon Dioxide. *Energy Environ. Sci.* **2010**, *3*, 43–81.
- (5) Olah, G. A.; Prakash, G. K. S.; Goepfert, A. Anthropogenic Chemical Carbon Cycle for a Sustainable Future. *J. Am. Chem. Soc.* **2011**, *133*, 12881–12898.
- (6) Appel, A. M.; Bercaw, J. E.; Bocarsly, A. B.; Dobbek, H.; DuBois, D. L.; Dupuis, M.; Ferry, J. G.; Fujita, E.; Hille, R.; Kenis, P. J. A.; et al. Frontiers, Opportunities, and Challenges in Biochemical and Chemical Catalysis of CO₂ Fixation. *Chem. Rev.* **2013**, *113*, 6621–6658.
- (7) Lu, Q.; Rosen, J.; Zhou, Y.; Hutchings, G. S.; Kimmel, Y. C.; Chen, J. G.; Jiao, F. A Selective and Efficient Electrocatalyst for Carbon Dioxide Reduction. *Nat. Commun.* **2014**, *5*, 3242.
- (8) Qiao, J.; Liu, Y.; Hong, F.; Zhang, J. A Review of Catalysts for the Electroreduction of Carbon Dioxide to Produce Low-Carbon Fuels. *Chem. Soc. Rev.* **2014**, *43*, 631–675.
- (9) η is defined as the difference between the thermodynamic potential for a CO₂ reduction process, E° , and the operating potential of the electrode, E , during catalysis.
- (10) Costentin, C.; Drouet, S.; Robert, M.; Savéant, J.-M. A Local Proton Source Enhances CO₂ Electroreduction to CO by a Molecular Fe Catalyst. *Science* **2012**, *338*, 90–94.
- (11) Schneider, J.; Jia, H.; Kobi, K.; Cabelli, D. E.; Muckerman, J. T.; Fujita, E. Nickel(II) Macrocycles: Highly Efficient Electrocatalysts for the Selective Reduction of CO₂ to CO. *Energy Environ. Sci.* **2012**, *5*, 9502–9510.
- (12) Bard, A. J.; Faulkner, L. R. *Electrochemical Methods: Fundamentals and Applications*, 2nd ed.; John Wiley & Sons, Inc.: New York, 2001.
- (13) Costentin, C.; Drouet, S.; Robert, M.; Savéant, J.-M. Turnover Numbers, Turnover Frequencies, and Overpotential in Molecular Catalysis of Electrochemical Reactions. Cyclic Voltammetry and Preparative-Scale Electrolysis. *J. Am. Chem. Soc.* **2012**, *134*, 11235–11242.
- (14) Wishart, J. F. Energy Applications of Ionic Liquids. *Energy Environ. Sci.* **2009**, *2*, 956–961.
- (15) Grills, D. C.; Fujita, E. New Directions for the Photocatalytic Reduction of CO₂: Supramolecular, scCO₂ or Biphasic Ionic Liquid-scCO₂ Systems. *J. Phys. Chem. Lett.* **2010**, *1*, 2709–2718.
- (16) *Ionic Liquids: Science and Applications*; Visser, A. E., Bridges, N. J., Rodgers, R. D., Eds.; ACS Symposium Series 1117; American Chemical Society: Washington, DC, 2013.
- (17) Rosen, B. A.; Salehi-Khojin, A.; Thorson, M. R.; Zhu, W.; Whipple, D. T.; Kenis, P. J. A.; Masel, R. I. Ionic Liquid-Mediated Selective Conversion of CO₂ to CO at Low Overpotentials. *Science* **2011**, *334*, 643–644.
- (18) Snuffin, L. L.; Whaley, L. W.; Yu, L. Catalytic Electrochemical Reduction of CO₂ in Ionic Liquid EMIMBF₄. *J. Electrochem. Soc.* **2011**, *158*, F155–F158.
- (19) Rosen, B. A.; Haan, J. L.; Mukherjee, P.; Braunschweig, B.; Zhu, W.; Salehi-Khojin, A.; Dlott, D. D.; Masel, R. I. In Situ Spectroscopic Examination of a Low Overpotential Pathway for Carbon Dioxide Conversion to Carbon Monoxide. *J. Phys. Chem. C* **2012**, *116*, 15307–15312.
- (20) DiMeglio, J. L.; Rosenthal, J. Selective Conversion of CO₂ to CO with High Efficiency Using an Inexpensive Bismuth-Based Electrocatalyst. *J. Am. Chem. Soc.* **2013**, *135*, 8798–8801.
- (21) Rosen, B. A.; Zhu, W.; Kaul, G.; Salehi-Khojin, A.; Masel, R. I. Water Enhancement of CO₂ Conversion on Silver in 1-Ethyl-3-Methylimidazolium Tetrafluoroborate. *J. Electrochem. Soc.* **2013**, *160*, H138–H141.
- (22) Salehi-Khojin, A.; Jhong, H.-R. M.; Rosen, B. A.; Zhu, W.; Ma, S.; Kenis, P. J. A.; Masel, R. I. Nanoparticle Silver Catalysts That Show Enhanced Activity for Carbon Dioxide Electrolysis. *J. Phys. Chem. C* **2013**, *117*, 1627–1632.
- (23) Sullivan, B. P.; Bolinger, C. M.; Conrad, D.; Vining, W. J.; Meyer, T. J. One- and Two-Electron Pathways in the Electrocatalytic Reduction of CO₂ by *fac*-Re(bpy)(CO)₃Cl (bpy = 2,2'-bipyridine). *J. Chem. Soc., Chem. Commun.* **1985**, 1414–1416.
- (24) Hawecker, J.; Lehn, J.-M.; Ziessel, R. Photochemical and Electrochemical Reduction of Carbon Dioxide to Carbon Monoxide Mediated by (2,2'-Bipyridine)tricarbonylchlororhenium(I) and Related Complexes as Homogeneous Catalysts. *Helv. Chim. Acta* **1986**, *69*, 1990–2012.
- (25) Babarao, R.; Dai, S.; Jiang, D.-e. Understanding the High Solubility of CO₂ in an Ionic Liquid with the Tetracyanoborate Anion. *J. Phys. Chem. B* **2011**, *115*, 9789–9794.
- (26) Mahurin, S. M.; Hillesheim, P. C.; Yeary, J. S.; Jiang, D.-e.; Dai, S. High CO₂ Solubility, Permeability and Selectivity in Ionic Liquids with the Tetracyanoborate Anion. *RSC Adv.* **2012**, *2*, 11813–11819.
- (27) Seki, S.; Serizawa, N.; Hayamizu, K.; Tsuzuki, S.; Umabayashi, Y.; Takei, K.; Miyashiro, H. Physicochemical and Electrochemical Properties of 1-Ethyl-3-Methylimidazolium Tris(pentafluoroethyl)-trifluorophosphate and 1-Ethyl-3-Methylimidazolium Tetracyanoborate. *J. Electrochem. Soc.* **2012**, *159*, A967–A971.
- (28) Barros-Antle, L. E.; Bond, A. M.; Compton, R. G.; O'Mahony, A. M.; Rogers, E. I.; Silvester, D. S. Voltammetry in Room Temperature Ionic Liquids: Comparisons and Contrasts with Conventional Electrochemical Solvents. *Chem.—Asian J.* **2010**, *5*, 202–230.
- (29) Pavlishchuk, V. V.; Addison, A. W. Conversion Constants for Redox Potentials Measured Versus Different Reference Electrodes in Acetonitrile Solutions at 25°C. *Inorg. Chim. Acta* **2000**, *298*, 97–102.
- (30) Meng, Y.; Aldous, L.; Belding, S. R.; Compton, R. G. The Hydrogen Evolution Reaction in a Room Temperature Ionic Liquid: Mechanism and Electrocatalyst Trends. *Phys. Chem. Chem. Phys.* **2012**, *14*, 5222–5228.
- (31) Meng, Y.; Aldous, L.; Belding, S. R.; Compton, R. G. The Formal Potentials and Electrode Kinetics of the Proton/Hydrogen Couple in Various Room Temperature Ionic Liquids. *Chem. Commun.* **2012**, *48*, 5572–5574.
- (32) Malherbe, C.; Robert, T.; Magna, L.; Olivier-Bourbigou, H.; Gilbert, B. Tentative Determination of the Acidity Level in Room Temperature Ionic Liquids by Electrochemical Methods. *ECS Trans.* **2009**, *16*, 3–16.
- (33) MacFarlane, D. R.; Vijayaraghavan, R.; Ha, H. N.; Izgorodin, A.; Weaver, K. D.; Elliott, G. D. Ionic Liquid “Buffers”-pH Control in Ionic Liquid Systems. *Chem. Commun.* **2010**, *46*, 7703–7705.
- (34) Barhdadi, R.; Troupel, M.; Comminges, C.; Laurent, M.; Doherty, A. Electrochemical Determination of pK_a of N-Bases in Ionic Liquid Media. *J. Phys. Chem. B* **2012**, *116*, 277–282.
- (35) Millán, D.; Rojas, M.; Santos, J. G.; Morales, J.; Isaacs, M.; Diaz, C.; Pavez, P. Toward a pK_a Scale of N-base Amines in Ionic Liquids. *J. Phys. Chem. B* **2014**, *118*, 4412–4418.
- (36) Rogers, E. I.; Silvester, D. S.; Poole, D. L.; Aldous, L.; Hardacre, C.; Compton, R. G. Voltammetric Characterization of the Ferrocene I Ferrocenium and Cobaltocenium I Cobaltocene Redox Couples in RTILs. *J. Phys. Chem. C* **2008**, *112*, 2729–2735.
- (37) Oldham, K. B.; Zoski, C. G. Comparison Of Voltammetric Steady States at Hemispherical and Disc Microelectrodes. *J. Electroanal. Chem.* **1988**, *256*, 11–19.
- (38) Janisch, J.; Ruff, A.; Speiser, B.; Wolff, C.; Zigelli, J.; Benthin, S.; Feldmann, V.; Mayer, H. A. Consistent Diffusion Coefficients of Ferrocene in Some Non-Aqueous Solvents: Electrochemical Simultaneous Determination Together With Electrode Sizes and Comparison to Pulse-Gradient Spin-Echo NMR Results. *J. Solid State Electrochem.* **2011**, *15*, 2083–2094.

- (39) Kaintz, A.; Baker, G.; Benesi, A.; Maroncelli, M. Solute Diffusion in Ionic Liquids, NMR Measurements and Comparisons to Conventional Solvents. *J. Phys. Chem. B* **2013**, *117*, 11697–11708.
- (40) Howell, J. O.; Wightman, R. M. Ultrafast Voltammetry and Voltammetry in Highly Resistive Solutions with Microvoltammetric Electrodes. *Anal. Chem.* **1984**, *56*, 524–529.
- (41) Heinze, J. Ultramicroelectrodes in Electrochemistry. *Angew. Chem., Int. Ed. Engl.* **1993**, *32*, 1268–1288.
- (42) The observation of catalytic CO₂ reduction at the first reduction wave in [emim][TCB] indicates that this is a two-electron reduction wave and that the value of the diffusion coefficient of **1** in [emim][TCB] that we measured by NMR and thus the resulting value of normalized current, $i/i_d = 2$ in Figure 1, is reasonable.
- (43) Electrocatalytic CO₂ reduction was previously reported at a silver electrode in H₂O with 18 mol % [emim][BF₄] (ref 17). However, we saw no current under CO₂ with a 0.5 mm silver disc electrode in [emim][TCB] containing 50 mM H₂O and no Re catalyst.
- (44) Silvester, D. S.; Uprety, S.; Wright, P. J.; Massi, M.; Stagni, S.; Muzzoli, S. Redox Properties of a Rhenium Tetrazolato Complex in Room Temperature Ionic Liquids: Assessing the Applicability of the Stokes-Einstein Equation for a Metal Complex in Ionic Liquids. *J. Phys. Chem. C* **2012**, *116*, 7327–7333.
- (45) Nicholson, R. S.; Shain, I. Theory of Stationary Electrode Polarography - Single Scan and Cyclic Methods Applied to Reversible, Irreversible, and Kinetic Systems. *Anal. Chem.* **1964**, *36*, 706–723.
- (46) Bard, A. J.; Faulkner, L. R. Electrode Reactions with Coupled Homogeneous Chemical Reactions. In *Electrochemical Methods: Fundamentals and Applications*; John Wiley & Sons, Inc.: New York, 2001; pp 471–533.
- (47) Dong, K.; Zhang, S.; Wang, D.; Yao, X. Hydrogen Bonds in Imidazolium Ionic Liquids. *J. Phys. Chem. A* **2006**, *110*, 9775–9782.
- (48) Silvester, D. S.; Compton, R. G. Electrochemistry in Room Temperature Ionic Liquids: A Review and Some Possible Applications. *Z. Phys. Chem.* **2006**, *220*, 1247–1274.
- (49) Tomita, Y.; Teruya, S.; Koga, O.; Hori, Y. Electrochemical Reduction of Carbon Dioxide at a Platinum Electrode in Acetonitrile-Water Mixtures. *J. Electrochem. Soc.* **2000**, *147*, 4164–4167.
- (50) Tachikawa, N.; Katayama, Y.; Miura, T. Electrode Kinetics of some Iron Complexes in an Imide-Type Room-Temperature Ionic Liquid. *J. Electrochem. Soc.* **2007**, *154*, F211–F216.
- (51) Hammouche, M.; Lexa, D.; Momenteau, M.; Savéant, J.-M. Chemical Catalysis of Electrochemical Reactions. Homogeneous Catalysis of the Electrochemical Reduction of Carbon Dioxide by Iron(0) Porphyrins. Role of the Addition of Magnesium Cations. *J. Am. Chem. Soc.* **1991**, *113*, 8455–8466.
- (52) Bhugun, I.; Lexa, D.; Savéant, J.-M. Catalysis of the Electrochemical Reduction of Carbon Dioxide by Iron(0) Porphyrins. Synergistic Effect of Lewis Acid Cations. *J. Phys. Chem.* **1996**, *100*, 19981–19985.
- (53) Fujita, E.; Chou, M.; Tanaka, K. Characterization of Ru-(bpy)₂(CO)(COO) Prepared by CO₂ Addition to Ru(bpy)₂(CO) in Acetonitrile. *Appl. Organomet. Chem.* **2000**, *14*, 844–846.
- (54) Părvulescu, V. I.; Hardacre, C. Catalysis in Ionic Liquids. *Chem. Rev.* **2007**, *107*, 2615–2665.
- (55) Zhang, J.; Bond, A. M. Practical Considerations Associated with Voltammetric Studies in Room Temperature Ionic Liquids. *Analyst* **2005**, *130*, 1132–1147.